arXiv:cond-mat/0509193v2 [cond-mat.mes-hall] 11 Sep 2005

Field sweep rate dependence of the coercive field of single-molecule magnets: a classical approach with applications to the quantum regime

W. Wernsdorfer[1], M. Murugesu[2], A.J. Tasiopoulos[2], and G. Christou[2]
[1]*Lab. L. Néel, associé à l'UJF, CNRS, BP 166, 38042 Grenoble Cedex 9, France*
[2]*Dept. of Chemistry, Univ. of Florida, Gainesville, Florida 32611-7200, USA*
(Dated: February 2, 2008)

A method, based on the Néel–Brown model of thermally activated magnetization reversal of a magnetic single-domain particle, is proposed to study the field sweep rate dependence of the coercive field of single-molecule magnets (SMMs). The application to Mn_{12} and Mn_{84} SMMs allows the determination of the important parameters that characterize the magnetic properties: the energy barrier, the magnetic anisotropy constant, the spin, τ_0, and the crossover temperature from the classical to the quantum regime. The method may be particularly valuable for large SMMs that do not show quantum tunneling steps in the hysteresis loops.

PACS numbers: 75.50.Xx, 75.75.+a, 75.45.+j, 75.50.Tt

I. INTRODUCTION

Single-molecule magnets (SMMs) exhibit slow magnetization relaxation of their spin ground state, which is split by axial zero-field splitting[1,2,3,4,5]. They are now among the most promising candidates for observing the limits between classical and quantum physics since they have a well defined structure, spin ground state and magnetic anisotropy. An important effort in synthetic chemistry has led to a quickly growing number of SMMs with an increasing number of magnetic centers. Recently, the molecular (or bottom-up) approach has reached the size regime of the classical (or top-down) approach to nanoscale magnetic materials[6]. Indeed, a giant Mn_{84} SMM was reported with a 4 nm diameter torus structure, exhibiting both magnetization hysteresis and quantum tunneling.

The study of such large systems is greatly complicated by the fact that the spin Hilbert space is huge and it is impossible to treat such systems with exact matrix diagonalization methods. However, since some SMMs are now as large as some classical nanoparticles, it raises the interesting possibility that classical models commonly employed to study the latter may be used to obtain a first-order understanding for large molecular systems. Indeed, we herein propose and demonstrate the use of the classical Néel–Brown model[7,8,9] of thermally activated magnetization reversal of a magnetic single-domain particle in order to study large SMMs. The proposed method allows us to determine important parameters that characterize the magnetic properties of the SMM: the energy barrier, the magnetic anisotropy constant, the spin, τ_0, and the crossover temperature from the classical to the quantum regime. The method is particularly useful for SMMs having low-lying energy states and not showing quantum tunneling steps in hysteresis loops. In such systems electron paramagnetic resonance (EPR) measurements often exhibit only very broad absorption peaks which do not allow the determination of the magnetic anisotropy.

In this letter, we apply the method to two systems whose properties are already known: (i) a Mn_{12} SMM with a well-characterized $S = 10$ ground state and (ii) a giant Mn_{84} SMM with $S = 6$ which has many low-lying energy states with higher spin values.

II. NÉEL–BROWN MODEL

The presented method is based on the Néel–Brown model of thermally activated magnetization reversal of a magnetic single-domain particle which has two equivalent ground states of opposite magnetization separated by an energy barrier due to magnetic anisotropy[7,8,9]. The system can escape from one state to the other either by thermal activation over the barrier at high temperatures or by quantum tunneling at low temperatures. At sufficiently low temperatures and at zero field, the energy barrier between the two states of opposite magnetization is much too high to observe an escape process. However, the barrier can be lowered by applying a magnetic field in the opposite direction to that of the particle's magnetization. When the applied field is close enough to the reversal field, thermal fluctuations are sufficient to allow the system to overcome the barrier, and the magnetization is reversed.

This stochastic escape process can be studied via the relaxation time method consisting of the measurement of the probability that the magnetization has not reversed after a certain time. In the case of an assembly of identical and isolated particles, it corresponds to measurements of the relaxation of magnetization. According to the Néel–Brown model, the probability that the magnetization has not reversed after a time t is given by:

$$P(t) = e^{-t/\tau} \tag{1}$$

and τ (inverse of the reversal rate) can be expressed by an Arrhenius law of the form:

$$\tau(T, H) = \tau_0 e^{\Delta E(H)/k_B T} \tag{2}$$

where $\Delta E(H)$ is the field dependent energy barrier height and τ_0 is the inverse of the attempt frequency. In most

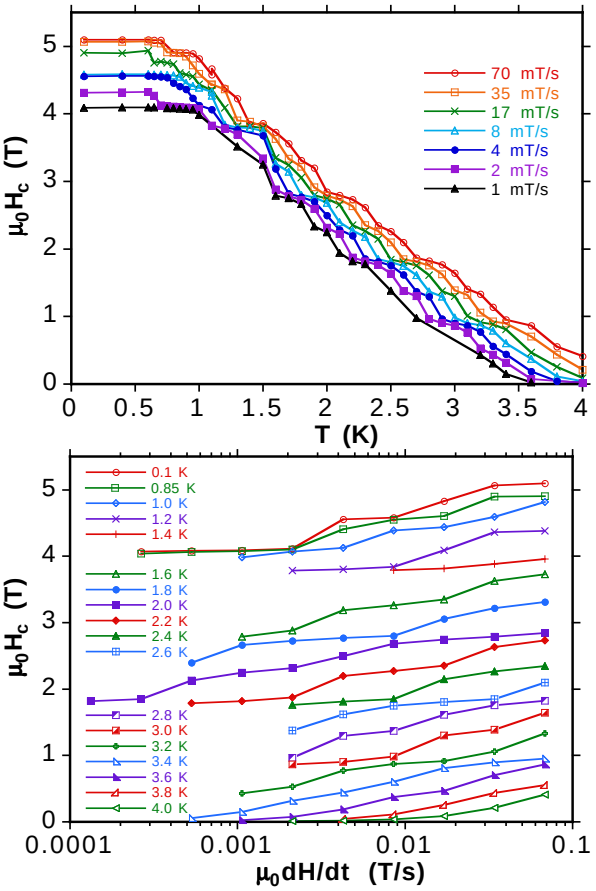

FIG. 1: (color online) Coercive field H_c for Mn_{12} as a function of (a) temperature and (b) field sweep rate. Note the steps of H_c coming from the resonant tunneling steps in the hysteresis loops.

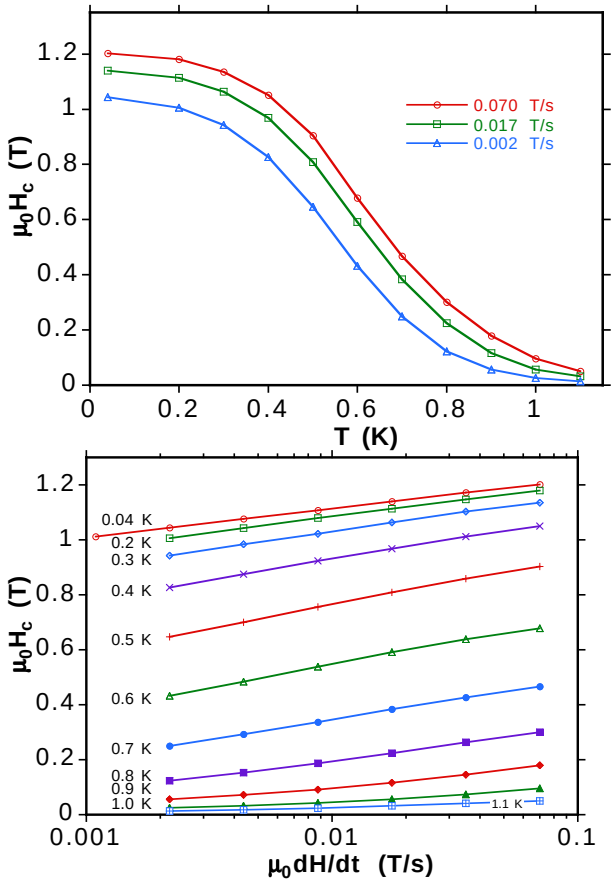

FIG. 2: (color online) Coercive field H_c for Mn_{84} as a function of (a) temperature and (b) field sweep rate.

cases, $\Delta E(H)$ can be approximated by

$$\Delta E(H) = E_0 \left(1 - H/H_c^0\right)^{\alpha} \qquad (3)$$

where H_c^0 is the reversal field at zero temperature, E_0 is the barrier height at zero applied field, and α is a constant of the order of unity (for most cases $1.5 \leq \alpha \leq 2$). In the case of a Stoner-Wohlfarth particle[10,11] with uniaxial anisotropy and the field applied along the easy axis of magnetization, all constants can be determined analytically[7,10]: $\alpha = 2$, $E_0 = KV$, and $H_c^0 = 2K/M_s$, where K is the uniaxial anisotropy constant, V is the particle volume, and M_s is the saturation magnetization. For SMMs with dominating uniaxial anisotropy: $\alpha = 2$, $E_0 = DS^2$, and $H_c^0 = 2DS/g\mu_0\mu_B$. However, in general, all constants depend slightly on fine details of the magnetic anisotropy and the direction of the applied field H[12,13].

In order to study the field dependence of the relaxation time $\tau(T, H)$ and to obtain the parameters of the model, the decay of magnetization has to be studied at many applied fields H and temperatures T. This is experimentally very time consuming and complicated by the fact that the equilibrium magnetization is temperature dependent and difficult to obtain for long relaxation times. In addition, for fast relaxation times the initial magnetization depends on the field sweep rates to apply the field. The number of exploitable decades for τ values is therefore limited for relaxation time measurements.

A more convenient method for studying the magnetization decay is by ramping the applied field at a given rate[14] and measuring the coercive field H_c (the field value to obtain zero magnetization), which is then measured as a function of the field sweep rate and temperature.

The mathematical transformation from a reversal time probability (Eqs. 1 and 2) to a reversal field probability was first given by Kurkijärvi[15] for the critical current in SQUIDs. Later, Gunther and Barbara calculated similar expressions for magnetic domain wall junctions[16]. A more general calculation was evaluated by Garg[17]. Here, we use a simplified version (see annex)[14] and approximate the mean reversal field of an assembly of identical particles or SMMs by the coercive field H_c:

$$H_c(T, v) \approx H_c^0 \left(1 - \left[\frac{kT}{E_0} \ln\left(\frac{c}{v}\right)\right]^{1/\alpha}\right) \qquad (4)$$

where the field sweeping rate is given by $v = dH/dt$; H_c^0 is the coercive field at zero temperature, and c depends on the details of the approximations: $c = H_c^0 k_B T/[\tau_0 \alpha E_0(1 - H_c/H_c^0)^{\alpha-1}]$ in reference[14], $c' = H_c^0(E_0/kT)^{1/\alpha}/(\tau_0\alpha)$ in reference[17], and it can be taken constant when the exact value of τ_0 is not needed. We applied the three approximations to nanoparticles[14] and here to SMMs and found that the first approximation gives a τ_0 which is closest to that extracted from an Arrhenius plot.

III. APPLICATION TO MN_{12} AND MN_{84}

In the present work, the method is applied to two SMMs: (i) $[Mn_{12}O_{12}(O_2CCH_2Bu^t)_{16}(CH_3OH)_4] \cdot CH_3OH$ and (ii) $[Mn_{84}O_{72}(O_2CMe)_{78}(OMe)_{24}(MeOH)_{12}(H_2O)_{42}(OH)_6]$, called respectively Mn_{12} and Mn_{84} henceforth. Full details of the synthesis, crystal structure and magnetic characterization are presented elsewhere[6,18].

The magnetization measurements were performed by using (i) a magnetometer consisting of several 6×6 μm^2 Hall-bars[19] and (ii) an array of micro-SQUIDs on top of which single crystals of Mn_{12} and Mn_{84} were placed, respectively. The field can be applied in any direction by separately driving three orthogonal superconducting coils. The field was aligned with the easy axis of magnetization using the transverse field method[20].

Typical hysteresis loops of both systems can be found elsewhere. Mn_{12} displays hysteresis loops with a series of quantum steps separated by plateaus[21] whereas Mn_{84} shows a smooth hysteresis without steps[6]. In order to apply the above method, the temperature and field sweep rate dependences of the coercive fields H_c were measured and plotted in Figs 1 and 2. Note that the curves for Mn_{12} show steps coming from the steps in the hysteresis loops[21]. As expected for a thermally activated process, H_c increases with decreasing temperature and increasing field sweep rate. Furthermore, all our measurements showed an almost logarithmic dependence of H_c on the field sweep rate (Figs. 1b and 2b). H_c becomes temperature independent below about 0.6 and 0.3 K, respectively for Mn_{12} and Mn_{84}.

The validity of Eq. 4 was tested by plotting the set of $H_c(T, v)$ values as a function of $[Tln(c/v)]^{1/2}$ where $c = H_c^0 k_B T/\tau_0 2E_0(1 - H_c/H_c^0)$. If the underlying model is sufficient, all points should collapse onto one straight line by choosing the proper values for the constant τ_0. We found that the data of $H_c(T, v)$ fell on a master curve provided $\tau_0 = 2.1 \times 10^{-7}$ s in Fig. 3 and 2×10^{-7} s in Fig. 4. Whereas for Mn_{84} the master curve is straight, it presents steps for Mn_{12}.

At low temperatures, strong deviation from the master curves are observed. In order to investigate the possibility that these low-temperature deviations are due to escape from the metastable potential well by tunneling, a common method for classical models is to replace the real

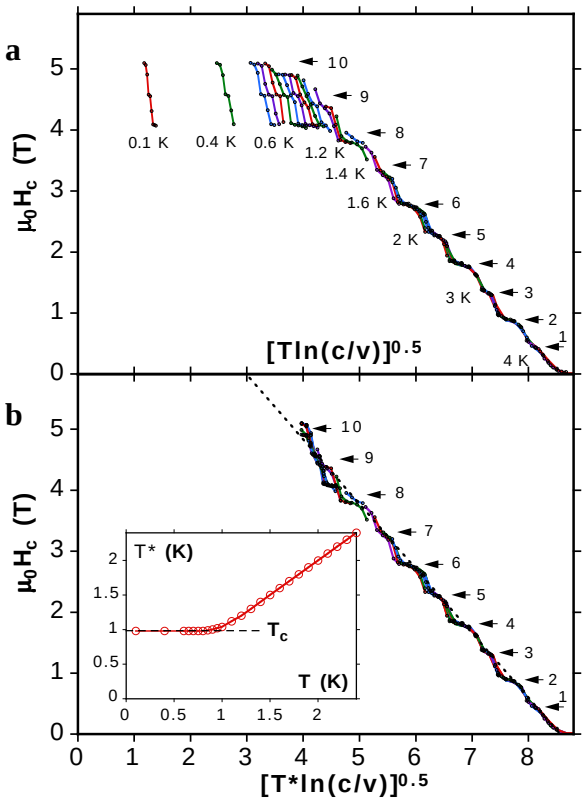

FIG. 3: (color online) (a) Scaling plot of the coercive field $H_c(T, v)$ of Mn_{12} for field sweep rates between 0.0001 and 0.1 T/s and several temperatures: 0.1 K, 0.4 K, from 0.6 to 1 K in steps of 0.05 K, and from 1 to 4 K in steps of 0.1 K. The arrows indicate the step index $n = -(m + m')$ where m and m' are the quantum numbers of the corresponding level crossing. Note the parity effect of the steps: even n have larger steps than odd n. (b) Same data of $H_c(T, v)$ and same scales but the real temperature T is replaced by an effective temperature T^* (see inset) which restores the scaling below 1.1 K.

temperature T by an effective temperature $T^*(T)$ in order to restore the scaling plot[22]. In the case of tunneling, $T^*(T)$ should saturate at low temperatures. Indeed, the ansatz of $T^*(T)$ as shown in the inset of Figs. 3b and 4b, can restore unequivocally the scaling plot demonstrated by a straight master curve (Figs. 3b and 4b). The flattening of T^* corresponds to a saturation of the escape rate, which is a necessary signature of tunneling. The crossover temperature T_c can be defined as the temperature where the quantum rate equals the thermal one. The inset of Figs. 3b and 4b gives $T_c = 0.97$ and 0.37 K for Mn_{12} and Mn_{84}, respectively. The slopes and the intercepts of the master curves give $E_0 = 72.4$ and 15.6 K and $H_c^0 = 9.1$ and 3.1 T, respectively for Mn_{12} and Mn_{84}. The E_0 values are in good agreement with those extracted from Arrhenius plots (69 K and 18 K for Mn_{12} and Mn_{84}, respectively)[6,18]. This result allows us to esti-

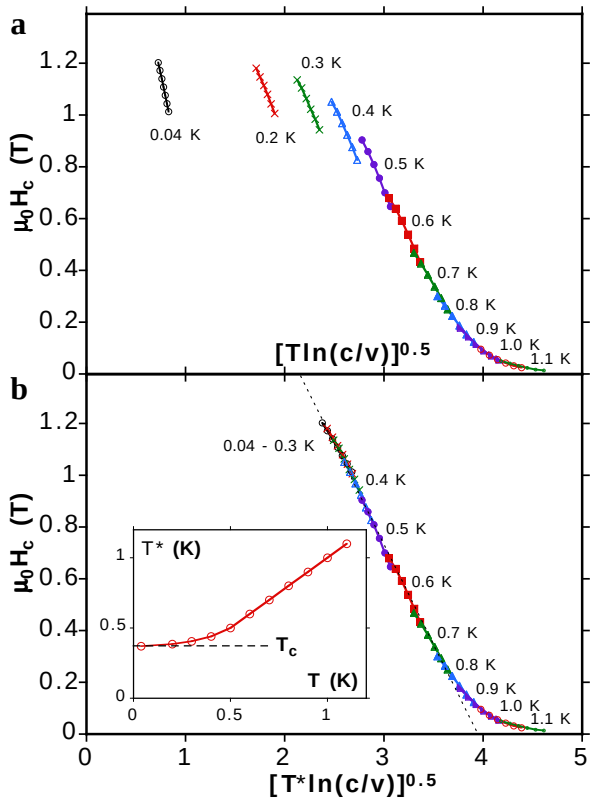

FIG. 4: (color online) (a) Scaling plot of the coercive field $H_c(T,v)$ of Mn_{84} for field sweep rates between 0.001 and 0.1 T/s and several temperatures (Fig. 2. (b) Same data of $H_c(T,v)$ but the real temperature T is replaced by an effective temperature T^* (see inset) which restores the scaling below 0.5 K.

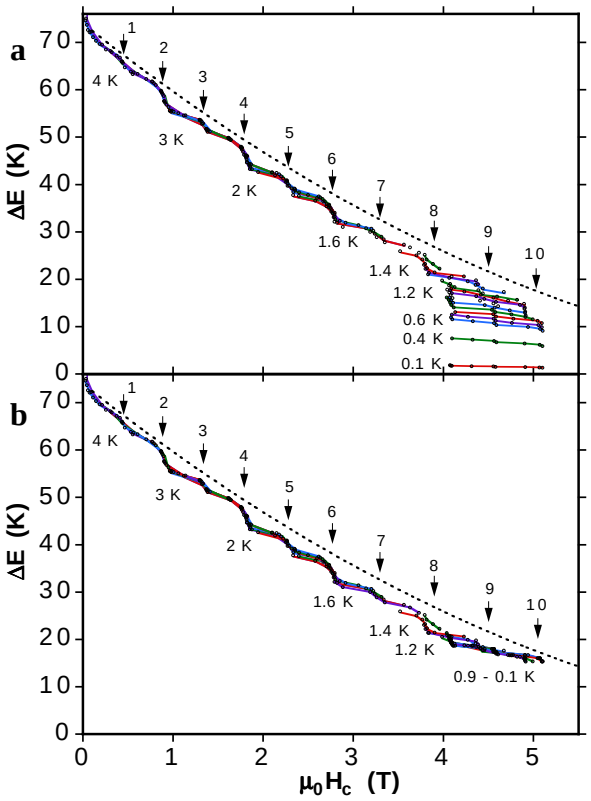

FIG. 5: (color online) (a) Field dependence of the energy barrier of Mn_{12} obtained from Eq. 8 and the set of $H_c(T,v)$ data from Fig. 3. The arrows indicate the step index $n = -(m+m')$ where m and m' are the quantum numbers of the corresponding level crossing. Note the step like reduction of the energy barrier due to resonant tunneling and the parity effect of the steps: even n have larger steps than odd n. The dotted line gives the classical barrier $\Delta E = E_0(1-H/H_a)^2$ with $E_0 = 74$ K and $H_a = 9.8$ T. (b) Same data of $H_c(T,v)$ but the real temperature T is replaced by an effective temperature T^* (see inset of Fig. 3b).

mate the spin ground state using $S = 2E_0/(g\mu_B\mu_0 H_c^0)$: S = 11 and 7 for Mn_{12} and Mn_{84}, respectively. This differs slightly from $S = 10$ and 6 determined via magnetization measurements. This deviation is due to quantum effects in the thermally activated regime and is considered further below.

Several points should be mentioned: (i) the classical regime of the model corresponds in most SMMs to the thermally activated tunneling regime with tunneling close to the top of the energy barrier. Because all parameters are deduced from this regime, small deviations from the exact values are expected; (ii) Eq. 4 is not valid for fields which are close to $H = 0$ because the model only takes into account the transitions from the metastable to the stable well. However, close to $H = 0$, transitions between both wells are possible leading to a rounding of the master curve at small fields; (iii) the method can be applied to powder samples with random orientations of the molecules. In this case, $\alpha \approx 1.5$, $\nu E_0 = DS^2$ where ν can be calculated[12,13], and the intercept of the master curve gives $H_c^0/2$; (iv) in the case of a distribution of anisotropies, different parts of the distribution can be probed by applying the method at different M values; (v) this method is insensitive to small intermolecular interactions when H_c is larger than the typical interaction field; and (vi) the method can be generalized for 1D, 2D, and 3D networks of spins. In this case, Eq. 3 describes a nucleation barrier.

IV. CONCLUSION

We introduce a method that uses the temperature and field sweep rate dependences of the coercive field of large SMMs in order to determine several parameters that characterize the magnetic anisotropy and the relaxation dynamics. We have succesfully applied the method to

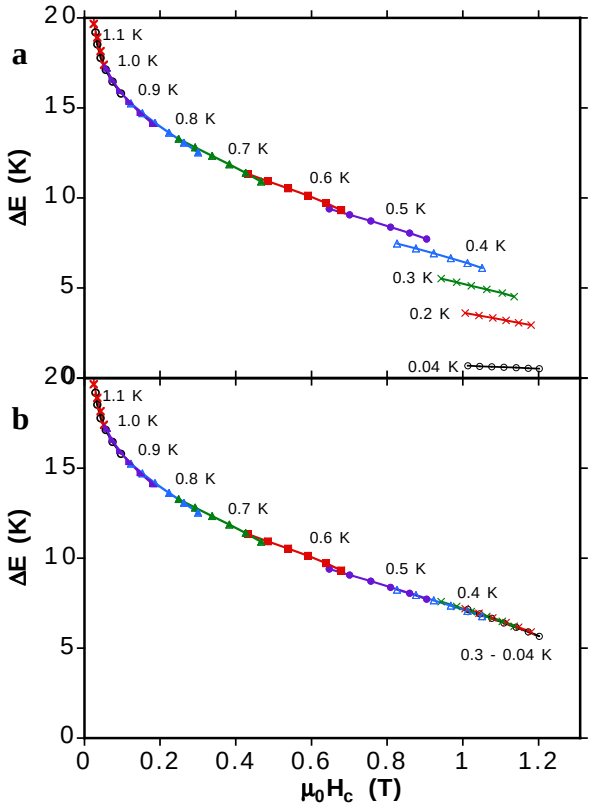

FIG. 6: (color online) (a) Field dependence of the energy barrier of Mn_{84} obtained from Eq. 8 and the set of $H_c(T, v)$ data from Fig. 4. (b) Same data of $H_c(T, v)$ but the real temperature T is replaced by an effective temperature T^* (see inset of Fig. 4b).

two test cases: (i) a Mn_{12} SMM with well known magnetic properties; and (ii) a giant Mn_{84} SMM which has many low-lying energy states with higher spin values. We believe that this method is an important tool to characterize magnetically new molecular systems of great complexity which do not allow a detailed undestanding on the quantum level.

This work was supported by the EC-TMR Network QuEMolNa (MRTN-CT-2003-504880), CNRS, Rhône-Alpes funding, and NSF.

V. ANNEX

The probability density of reversal of a stochastic process is

$$-\frac{dP}{dt} = \frac{1}{\tau}P \tag{5}$$

and the maximum of the probability density can be derived from

$$\frac{d^2P}{dt^2} = \frac{P}{\tau^2}\left(1 + \frac{d\tau}{dt}\right) = 0 \tag{6}$$

This gives the following general result for the maximum of the probability density

$$\frac{d\tau}{dt} = -1 \tag{7}$$

The application of the result to Eq. 2 leads to

$$\Delta E(H) = k_B T \ln\left(\frac{k_B T}{\tau_0 \frac{dE}{dH}\frac{dH}{dt}}\right) \tag{8}$$

Using Eqs. 3 and 8, we find Eq. 4.

Eq. 8 can be used to plot directly the field dependence of the energy barrier (Figs. 5 and 6)

[1] R. Sessoli, H.-L. Tsai, A. R. Schake, S. Wang, J. B. Vincent, K. Folting, D. Gatteschi, G. Christou, and D. N. Hendrickson, J. Am. Chem. Soc. **115**, 1804 (1993).
[2] R. Sessoli, D. Gatteschi, A. Caneschi, and M. A. Novak, Nature **365**, 141 (1993).
[3] G. Christou, Polyhedron XX, XXX (2005).
[4] N. Aliaga-Alcade, R.S. Edwards, S.O. Hill, W. Wernsdorfer, K. Folting and G. Christou, J. Am. Chem. Soc. 126, 12503 (2004).
[5] N. E. Chakov, M. Soler, W. Wernsdorfer, K.A. Abboud, and G. Christou, Inorg. Chem. 44, 5304 (2005).
[6] A.J. Tasiopoulos, A. Vinslava, W. Wernsdorfer, K.A. Abboud, and G. Christou, Angew. Chem. Int. Ed. Engl. **43**, 2117 (2004).
[7] L. Néel, Ann. Geophys. **5**, 99 (1949).
[8] W. F. Brown, Phys. Rev. **130**, 1677 (1963).
[9] W. T. Coffey, D. S. F. Crothers, J. L. Dormann, Yu. P. Kalmykov, , and J. T. Waldron, Phys. Rev. B **52**, 15951 (1995).
[10] L. Néel, C. R. Acad. Science **224**, 1550 (1947).
[11] E. C. Stoner and E. P. Wohlfarth, Philos. Trans. London Ser. A **240**, 599 (1948), reprinted in IEEE Trans. Magn. MAG-27, 3475 (1991).
[12] A. Thiaville, J. Magn. Magn. Mat. **182**, 5 (1998).
[13] A. Thiaville, Phys. Rev. B **61**, 12221 (2000).
[14] W. Wernsdorfer, E. Bonet Orozco, K. Hasselbach, A. Benoit B. Barbara, N. Demoncy, A. Loiseau, D. Boivin, H. Pascard, and D. Mailly, Phys. Rev. Lett. **78**, 1791 (1997).
[15] J. Kurkijärvi, Phys. Rev. B **6**, 832 (1972).
[16] L. Gunther and B. Barbara, Phys. Rev. B **49**, 3926 (1994).
[17] A. Garg, Phys. Rev. B **51**, 15592 (1995).
[18] M. Murugesu and et al., to be submitted (2005).
[19] L. Sorace, W. Wernsdorfer, C. Thirion, A.-L. Barra, M. Pacchioni, D. Mailly, and B. Barbara, Phys. Rev. B **68**, 220407(R) (2003).
[20] W. Wernsdorfer, N. E. Chakov, and G. Christou, Phys. Rev. B **70**, 132413 (2004).

[21] W. Wernsdorfer, M. Murugesu, and G. Christou, cond-mat/0508437 .
[22] W. Wernsdorfer, E. Bonet Orozco, K. Hasselbach, A. Benoit, D. Mailly, O. Kubo, H. Nakano, and B. Barbara, Phys. Rev. Lett. **79**, 4014 (1997).